Comparison of Full-Scale and Wind-Tunnel Studies of a Separation Bubble

Z. Zhao[1], P.P. Sarkar[1], R.N. Meroney[2], D.E. Neff[2] and D. Banks[2]

1 Wind Engineering Research Center, Department of Civil Engineering, Texas Tech University, Lubbock, TX 79409-1023/
2 Fluid Mechanics and Wind Engineering Program, Civil Engineering Department, Colorado State Univ., Fort Collins, CO 80523

Abstract

The mean structure of the separation bubble over roof of the Texas Tech Experimental Building is established from full-scale velocity measurements and compared with that obtained in a wind tunnel. Pressure acting on the roof is measured and it is found that the mean pressure distribution is closely related to the flow structure. Effort is made to understand the mechanism of peak-pressure generation. A non-conventional pressure coefficient is introduced to possibly separate the effects of the wind speed magnitude from that of the wind direction. Roof pressure along with wind speed and direction immediately upstream of the building were simultaneously recorded and examined. It is observed that large-and-fast fluctuations in the upstream wind direction about the wall-normal are closely associated with low non-conventional pressure coefficient values. For the conventional pressure coefficient, the effect of fluctuations of the upstream wind speed on roof pressure is observed to be quasi-steady, the main contribution to the rms of Cp is from the wind magnitude fluctuation. The non-conventional Cp could assume values significantly lower than what has been documented for the conventional Cp, if strong gusts could concur with large-and-fast fluctuations in wind direction.

1. Introduction

Comparison of pressure data between wind-tunnel and full-scale studies for flow around low buildings has been of special interest in the recent past ([1], [2] and others). It was observed that the values of peak and rms pressure coefficients for the worst-suction taps are consistently lower in the wind-tunnel tests than those seen in full-scale tests. Various theories, including the effects of Reynolds number and small-scale turbulence, have been suggested to explain these differences. To better understand the flow mechanism in the separated flow regions that produce these worst negative pressures, Colorado State University (CSU) and Texas Tech University (TTU) are conducting experiments in both wind-tunnel model scale (CSU) and full scale (TTU) under the CSU/TTU Cooperative Program in Wind Engineering (CPWE). This is a five-year (1995-1999) research program, completion of which will eventually lead to a better explanation of the peak-load generating mechanism and provide data that will result in improved wind-tunnel simulation and computational methods. Investigation of the wind flow about low buildings is one of the three major emphasis areas in this cooperative research. Mainly two flow cases are being investigated; flow normal to the walls of the TTU building producing separated flow on the roof, and flow at oblique angles with respect to these walls producing corner roof vortices. Visualization and measurement of flow and its correlation with pressure fluctuations and characteristics of the approaching wind are of interest in this study. In this paper, detailed full-scale studies at TTU and its comparison with the wind-tunnel studies at CSU for flow approaching normal to a building wall are discussed. The goal of this paper is to document the flow characteristics of the separation bubble (SB) and to find its relationship with the upstream wind and its effects on the pressure fluctuations.

The separation bubble and the external roof-pressure characteristics associated with the vortex circulation within the bubble are worth investigating, from the viewpoint of both academic interest and practical importance. Field surveys of building damage inflicted by severe winds indicate that the roof-eaves regions and the roof-corner regions are among the most vulnerable zones in a building envelope. When wind approaches a building normal to one of its walls, the flow can not negotiate the sharp roof edge because of its viscosity. Thus, it separates to form a shear-layer which may re-attach to create a SB. Peak pressure coefficients measuring up to -9 have been documented in full-scale measurements under the SB. The corresponding values for pressures induced by conical vortices at roof corners are slightly higher but comparable in magnitude. However, these are two distinct flow phenomena. The separation bubble is not a special case of the conical vortex at a specific wind angle because worst suctions for the eaves areas and the roof corners do not occur at the same building orientation with respect to the upstream wind.

In a related paper by Sarkar et. al. [3], flow visualization techniques and flow measurement equipment suitable for full-scale applications were discussed in detail. Employing flow visualization techniques, some preliminary observations were made about the dynamics of the separation bubble; velocity profiles for the separation bubble were obtained from flow measurement using a two-component sonic anemometer [3]. In this study, results of more refined flow measurements will be discussed. A three-component ultrasonic anemometer was incorporated into the existing data acquisition system to facilitate simultaneous measurement of wind flow on the roof along with the surface pressures.

2. Method

2.1 Flow Visualization

Three different methods have been successfully employed at TTU for flow visualization in full scale [3]. These methods are the tuft-grid method, the smoke injection technique and the airfoil-grid method. In all the three cases, visualizations were more effective at night when flood lights were used for illumination. An 8-mm videocam was used to record the flow in each method. In the tuft-grid method, a 20 ft x 7 ft metal frame with a 6-in. grid was used. Colored yarn segments tied to the nodes of this grid aided in the visualization process. A high-performance smoke generator (IF-100), along with a number of smoke bombs tied to a metal grid placed along the centerline of the building, was used for visualization in the smoke-injection technique. The airfoil-grid is a relatively new method for full-scale applications. Several light-weight airfoils made out of Balsa wood and 80-lb paper were fixed to a metal grid such that they were free to rotate in the plane of the grid. Reflective tape on the side of the airfoils was used to aid visualization at night.

Flow visualization on a TTU building model at CSU involved a Coherent Innova 70-5 Argon-ion water cooled laser operating in multi-line mode. The laser beam was reflected and spread into a sheet by lenses mounted on the wind-tunnel ceiling. The light sheet was aligned along the centerline of the model. Glycerin smoke was introduced for visualization with the light sheet that was recorded on an SVHS camera.

2.2 Flow-Measurement Setup

Direct and systematic flow measurements of velocities within the SB were carried out separately as well as simultaneously with flow visualization, approaching-flow measurement and pressure measurements. The Texas Tech Experimental Building or the WERFL (Wind Engineering Research Field Laboratory) is a rectangular building with a flat roof located in an open-flat terrain. It has a dimension of 9.1 m (B) x 13.7 m (L) x 4.0 m (H) (30x45x13 ft). Flow measurements in this study were carried out along the short-roof axis (9.1m). The upstream wind velocities were measured by UVW anemometers at different heights of a 49-m meteorological tower that is located 46 m west of the building. The three-component ultrasonic anemometer (Model 1210R3, Gill Instruments Ltd.) samples an air volume of about 852 cm^3 (a cylinder with a diameter of 10.2 cm and a

height of 10.5 cm) that is enclosed by three pairs of probes. The separation between the two opposite probes of each pair is 14.6 cm. The spatial resolution of the ultrasonic anemometers compares very well with wind-tunnel measurements by hot-film probes on geometrically-scaled models (usually 1:50 or 1:100 scale). None of the probe-pair axes align with the principal flow direction. The sonic anemometer measures the velocities along the three probe axes and then these values are converted to the conventional u, v and w velocity components. Since the flow inside the separation bubble is highly turbulent with frequent flow reversals in all three directions, flow measurement using ordinary hot-wire anemometers would be impossible because of their flow-direction ambiguity. Sonic anemometers seem to be the only feasible option for this full-scale application. One sonic anemometer was used for the entire experiment; the anemometer was mounted on a portable support and set to a desired position manually. The sampling frequency was 30 Hz which was the same as that of pressure measurement; the duration of each run was fifteen minutes.

3. Structure of the Separation Bubble

Each data run (Mode 49) simultaneously recorded u, v and w components of flow velocity at one particular location within the separation bubble (SB), upstream flow velocities at the meteorological tower and roof pressures along the short building axis. The sonic wind speeds were normalized with the corresponding upstream mean-wind velocity simultaneously measured at the roof-height (4.0 m) level. Data from each of these 103 runs were analyzed to obtain the normalized mean wind velocity vectors at various locations within the SB. A sketch of the mean structure of the separation bubble that is created with these normalized velocity vectors is plotted in Fig. 1; while some detailed statistics are listed in Table 1 for the purpose of comparison by other researchers. For plotting, all lengths of the velocity vector were scaled with that of the longest one which was assigned a convenient size. In Table 1, x is the distance from the leading edge, h is the height above roof, α is the angle of the velocity vector with respect to the normal to the windward wall, and *vel.* represents the mean flow speed on the roof as a fraction of the upstream mean velocity at the roof height.

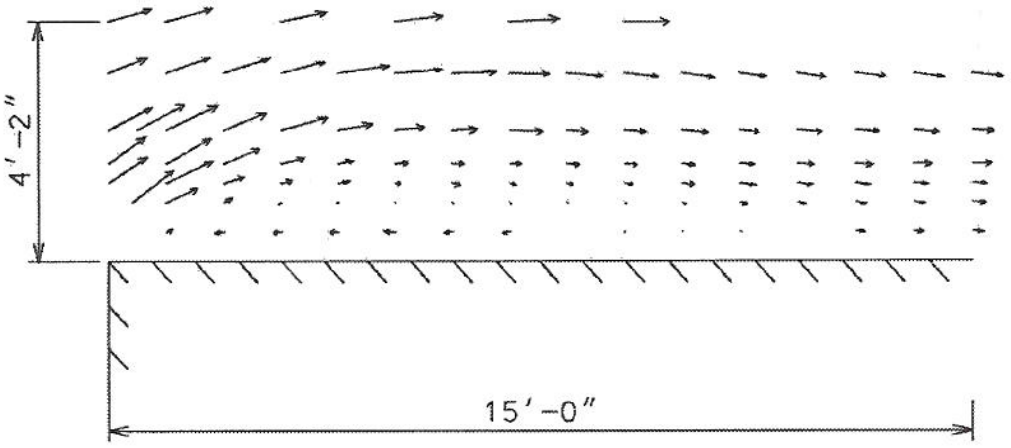

Figure 1. Mean-structure of the separation bubble as depicted by the mean-velocity vectors

A few observations can be made about the time-averaged SB. The vortex is quite elongated along the horizontal dimension. The mean reattachment point is identified by a nearly downward pointing velocity vector located at about 3.05 m from the leading edge. The region with predominant flow reversal was very much confined close to the roof surface. In this region, the time-series record indicates frequent flow reversals and the mean speeds were low. The time-averaged structure of this core region of the vortex within the SB presents a picture of stillness. In the immediate proximity of the roof along the building axis, there exists three distinct

zones: a flow reversal zone near the leading edge followed by a reattachment zone and a forward flow zone, all in the sense of averaging. Away from the leading edge, some amount of flow reversal was present at the highest level where flow was measured in this study and was expected to exist even at a slightly greater height until the boundary of the SB. The intermittency factor as defined in [3] is the fraction of the time the local flow is reverse of the upstream flow direction. An intermittency factor of one or two percent could be chosen to determine the vertical dimension of the separation bubble. Despite the randomness and the turbulent nature of the flow inside the SB, its averaged structure is amazingly organized and regular to small details.

Table-1 Statistics of velocity vectors

h= 0.15 m (0'-06")				**h= 0.30 m (1'-00")**			
Run #	x in m (ft)	α (deg.)	vel.	Run #	x in m (ft)	α (deg.)	vel.
9	0.13 (0'-05")	139.8		13	0.13 (0'-05")	142.4	1.182
49	0.30 (1)	166.5	0.087	14	0.30 (1)	155.8	0.787
48	0.61 (2)	-5.8	0.146	15	0.61 (2)	154.7	0.125
47	0.91 (3)	-4.5	0.187	16	0.91 (3)	-31.3	0.063
46	1.22 (4)	-1.4	0.200	18	1.22 (4)	-11.5	0.052
45	1.52 (5)	-0.5	0.210	19	1.52 (5)	-56.5	0.018
44	1.83 (6)	-5.9	0.143	20	1.83 (6)	-96.7	0.029
43	2.13 (7)	-6.6	0.119	22	2.13 (7)	-96.6	0.030
38	2.44 (8)	-8.4		23	2.44 (8)	-118.9	0.045
37	2.74 (9)	-63	0.030	24	2.74 (9)	-143.8	0.077
36	3.05 (10)	-89.5	0.018	25	3.05 (10)	-158.2	0.119
35	3.35 (11)	-153.3	0.038	204	3.35 (11)	-162.8	0.110
31	3.66 (12)	-171.6		205	3.66 (12)	-168.5	0.155
30	3.96 (13)	-174.8	0.148	206	3.96 (13)	-170.0	0.183
29	4.27 (14)	-176.8	0.203	207	4.27 (14)	-175.2	0.277
26	4.57 (15)	-175.9	0.214	208	4.57 (15)	-175.4	0.258
h=0.69 m (2'-03")				**h=0.91m (3'-0")**			
72	0.00 (0')	152.4	1.139	105	0.00 (0')	158.6	0.962
73	0.15 (0'-06")	151.42	1.234	106	0.15 (0'-06")	160	
74	0.30 (1)	154.04	1.312	107	0.30 (1)	160.6	1.080
81	0.61 (2)	157.94	1.078	108	0.61 (2)	162.4	1.127
82	0.91 (3)	164.63	1.113	109	0.91 (3)	165.9	1.052
84	1.22 (4)	169.93	0.816	112	1.22 (4)	171.8	1.204
88	1.52 (5)	173.66	0.672	113	1.52 (5)	175.3	1.094
92	1.83 (6)	177.31	0.571	115	1.83 (6)	178.6	1.017
94	2.13 (7)	-178.23	0.601	116	2.13 (7)	-178.8	0.916
95	2.44 (8)	-175.7	0.488	117	2.44 (8)	-176.1	0.833
97	2.74 (9)	-174.96	0.508	119	2.74 (9)	-174.7	0.769
98	3.05 (10)	-175.38	0.606	120	3.05 (10)	-172.6	0.741
99	3.35 (11)	-175.25	0.440	121	3.35 (11)	-172.5	0.633
100	3.66 (12)	-175.51	0.546	122	3.66 (12)	-171.9	0.645
101	3.96 (13)	-175.28	0.542	126	3.96 (13)	-173.7	0.703
103	4.27 (14)	-174.77	0.573	127	4.27 (14)	-172.9	0.712
104	4.57 (15)	-177.03	0.486	128	4.57 (15)	-174.1	0.709

4. Mean Pressure Distribution

Pressure data (Mode 49) from six pressure taps along the short axis of the roof were available for analysis. These taps are 50223, 50523, 50923, 51423 and 52923; data for tap 50123 were from Mode 15. Their location and the mean pressure coefficient (C_P) are listed in Table 2.

Table 2. Location of pressure taps and mean pressures

Tap No.	Location		Cp (Mean)	Remarks
	x (m)	y (m)		
50123	0.31	7.06	-1.18	Mode-15 data
50223	0.51	7.06	-1.05	Mode-49 data
50523	1.42	7.06	-0.73	
50923	2.64	7.06	-0.72	
51423	4.32	7.06	-0.43	Reattachment
52323	6.88	7.06	-0.25	occurs at 3.05 m
52923	8.92	7.06	-0.21	

Since the mean reattachment point is at about 3.05 m from the leading edge, taps 50123, 50223, 50523 and 50923 are located upstream of the reattachment point while taps 51423, 52323 and 52923 are downstream of the reattachment point. A closer look at the velocity vectors near the leading edge of the roof reveals that taps 50123 and 50223 are in the wedge-shaped region (Fig. 2). These taps record the strongest suction that can be possibly explained by a vacuum-like effect, i.e. the air pocket within the wedge-shaped region (Fig. 2) is forced to go upward by the forward and reverse flows to create a zone of extremely high suction. Tap 50223 appears to be in the vicinity of a reverse stagnation point ($C_P \approx -1.0$) where a streamline originates and moves upward along with the rest of the flow (shown as a dashed line in Fig. 2).

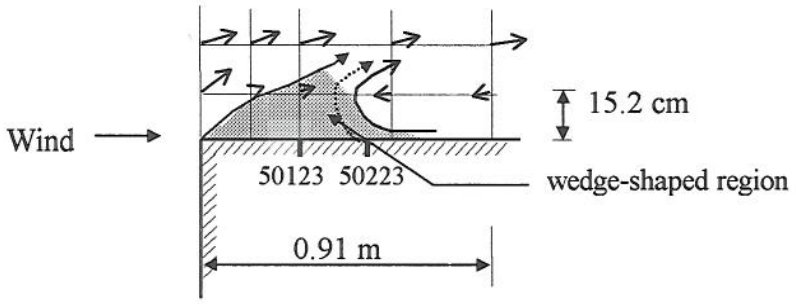

Figure 2: Structure of the flow near the leading edge of the separation bubble

Taps 50523 and 50923 are located within the zone of flow reversal and their mean pressures differ slightly. Taps 52323 and 52923 are located in the forward flow region and their mean pressures differ by a small amount that can be explained by the increase in mean flow velocity near the roof from tap 52323 to tap 52923. Tap 51423 records a mean pressure that falls somewhere in between the values of these two distinct regions.

5. Peak-Pressure Generating Mechanism

Runs 72, 105, 213 of the Mode-49 data were used for the analysis. In these runs, the sonic anemometer was set right above the leading roof edge at heights of 0.69 m (2'-03"), 0.91 m (3') and 1.27 m (4'-02''), respectively. It was used to measure wind that is later referred as upstream wind for characterizing the pressures.

The location of the sonic anemometer at the leading edge was required to precisely find the effect of the wind direction on the roof pressures underneath the SB. Also, the UVW anemometer could not have captured a fast rate of change in the wind direction. A 'non-conventional' pressure coefficient (C_P) is introduced here. It is defined as the ratio of the surface pressure to the instantaneous dynamic pressure ($\rho V^2(t)/2$) instead of the mean dynamic pressure ($\rho \overline{V}^2/2$) of the undisturbed flow upstream of the building. The introduction of the non-conventional pressure coefficient makes it possible to isolate the effects of the wind direction fluctuation from those of the wind speed fluctuation on the mechanism of pressure generation. To obtain the non-conventional pressure coefficients, instantaneous dynamic pressures with corrected values of wind speeds measured by the sonic anemometer were used. This correction was required because of the effect of acceleration of the flow above the leading roof edge. The correction factor used was the ratio of the run-averaged speeds of the sonic anemometer to that measured by the UVW anemometer on the meteorological tower at the roof level (4m). Comparison of data between the sonic and the UVW anemometers indicated that the wind direction given by the latter accurately represented the wind direction of the undisturbed upstream flow. Some statistics of the upstream wind measured on the meteorological tower are listed in Table 3. In each run case, the wind was nearly normal to the long-wall of the building.

Table 3. Statistics of upstream wind at roof level

Run	azimuth wind direction in degrees					magnitude in m/s (mph)			
	mean	rms	min.	max.	range	mean	rms	min.	max.
72	142.7	8.78	116.5	175.3	58.7	6.4 (14.3)	1.47 (3.3)	2.10 (4.7)	12.8 (28.6)
105	230.6	10.9	194.3	264.5	70.2	8.2 (18.3)	1.8 (4.1)	3.5 (7.9)	15.1 (33.7)
213	236.3	9.31	205.0	266.6	61.6	10.4 (23.3)	2.3 (5.1)	4.6 (10.4)	21.1 (47.2)

It was noticed that natural wind changes direction and speed considerably, characteristics not adequately simulated in wind-tunnels. Past records at WERFL showed that within a time period of 15 minutes wind direction fluctuation in the range of 70 degrees is common and large changes in wind direction can occur in a very short-time period. Direction fluctuation of as large as 90 degrees in one tenth of a second was observed at 20 mph or even higher wind speeds. Compared with the rate of wind direction fluctuations, the rate of wind speed fluctuation was observed to be slower.

Extensive comparison of time series of the upstream wind speed and direction with those of the conventional and the non-conventional pressure coefficients (tap 50223) were conducted. Due to space limitation only one representative segment of 1-minute duration is shown in Fig. 3 to illustrate some of the following observations.

When the direction is not fluctuating much, lower-than-mean wind speeds were responsible for small conventional C_P values (less suctions) within a run simply because of its definition; suction peaks often concurred with upstream wind gusts. Conventional C_P peaks also occurred with large-and-fast change in upstream wind direction (about the mean) in spite of lower-than-mean wind speeds (a peak in the non-conventional C_P; t = 662, 711 sec., Fig. 3); and sometimes the peaks over one run were likely to be the combined results of a gust and a large-and-fast wind direction fluctuation about the normal (t = 668 sec., Fig. 3).

Large-and-fast fluctuations of wind direction about the wall-normal were responsible for peaks of non-conventional C_P (t = 662, 711 sec., Fig. 3). Because of the characteristics of natural wind, which has significant longitudinal-speed fluctuations but less frequent fluctuations in direction within a very short time period, the conventional C_P is much more dynamic than the non-conventional C_P which looks flatter. In the same sense, the conventional C_P usually has more local peaks and the non-conventional C_P has fewer but more distinct peaks.

It is worth noting that the mean pressure coefficients within the separation bubble at tap 50223 along the short axis are not sensitive to the mean wind directions; only marginal change of mean pressures were observed (-1.0 to -1.5) for upstream wind directions ranging between plus and minus 45 degrees from the normal direction. Hence, the generation of peak pressures of -4.8 (conventional C_P) in this run can not be explained by the mean pressure versus wind angle relationship. Short-lasting C_P peaks seemed to occur whenever there was a large-and-fast fluctuation of wind direction about the windward wall normal.

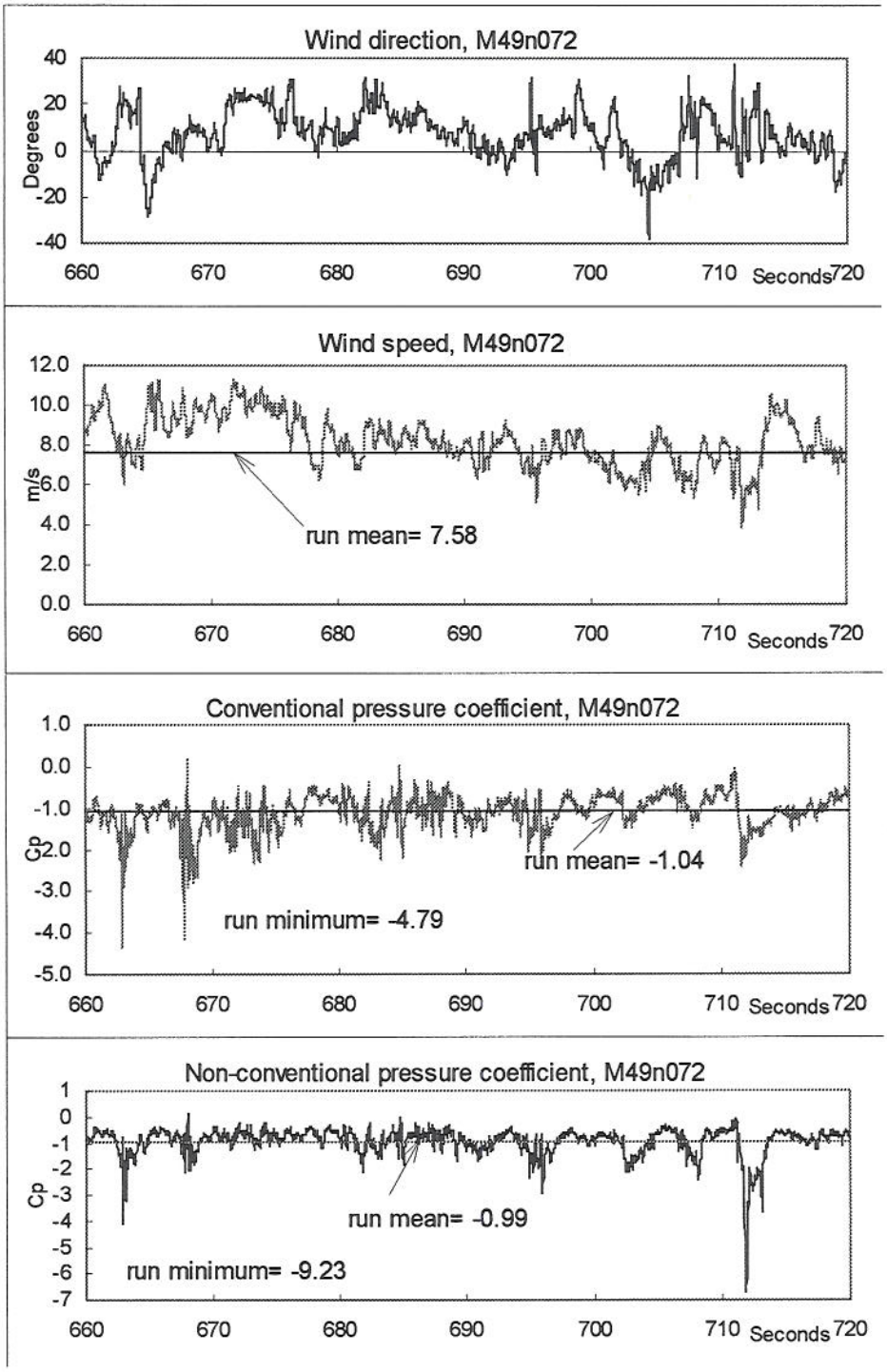

Figure 3. Time series comparison of upstream wind and pressure coefficient at tap 50223

6. Conclusion

The mean roof pressure distribution underneath the SB is directly related to the flow structure within the SB. The separation bubble is quite elongated in the horizontal direction and confined close to the roof. Within the SB four flow zones could be identified near the roof: (1) a leading-edge zone, where the separated shear-layer meets with the reverse flow to create a wedge-shaped region having maximal suction; (2) a reverse-flow zone; (3) a reattachment zone; and (4) a forward-flow zone. On a flat-roof, the suction decreases with distance from the leading edge and the pressure distribution is quite uniform within each zone.

With the introduction of the non-conventional C_P, the effects of the magnitude and the direction of upstream wind on roof pressure developed under the SB could be separated. The non-conventional C_P has fewer and more distinct peaks as a result of lesser frequent changes in wind direction. By using the instantaneous upstream velocity, the non-conventional C_P is more consistent and reveals the mechanism of pressure generation.

Actually, time-series analysis indicates that large-and-fast direction fluctuation in natural wind governs the mechanism of peak-pressure generation. This is probably related to the fact that the reattachment process depends on the mass balance within the SB [4] which is a two-dimensional and unstable flow phenemenon when upstream wind is normal to the windward wall. Large-and-fast fluctuations of wind direction about this normal seem to disturb this delicate balance in the SB following which a high suction is induced. The exact mechanism inside the SB is not clear at this point. However, the conical vortex that also involves flow separation and reattachment is highly stable [4]. While ultimate peaks of conventional C_P were often associated with large-and-fast direction fluctuations about the windward wall normal, gusts were generally responsible for the fluctuations and the secondary peaks and hence the rms values.

If the above observations are verified by other researchers, the implications are significant. First, improvement in wind-tunnel simulations to predict peak pressures could be achieved, if new techniques could be developed to generate gustier wind with considerable and fast fluctuation in wind direction; for design purposes, at the same design wind speed, higher magnitude peak pressures than those obtained by the peak conventional C_P values could be possible, if a strong gust concurrently occurs with large-and-fast fluctuations in wind direction. If this is true then the use of non-conventional peak C_P is justified for design instead of the conventional peak C_P.

7. Acknowledgment

The work cited is based upon one of the three technical topics being studied under the Colorado State University/Texas Tech University Cooperative Program in Wind Engineering. The financial support for this work from the US National Science Foundation (Grant No. CMS-9411147 and CMS-9409869) is appreciated.

8. References

[1] Cochran L.S. (1992). "Wind-tunnel modeling of low-rise structures," *Ph.D. dissertation*, Civil Engineering Department, Colorado State University.

[2] Tieleman H.W. (1994). "Model/full scale comparison of pressures on the roof of the TTU experimental building," *Proceedings of the East European Conference on Wind Engineering*, Warsaw, Poland.

[3] Sarkar P.P., Zhao Z., and Mehta K.C. (1996). "Flow Visualization and measurement on the roof of the Texas Tech Building," *Proceedings of the Third International Colloquium on Bluff Body Aerodynamics and Applications*, Blacksburg, Virginia, July (1996), Accepted for publication in the *J. Wind Eng. and Indust. Aero*.

[4] Kind, R. J. (1986). "Worst suctions near edges of flat rooftops on low-rise buildings," *Journal of Wind Engineering and Industrial Aerodynamics*, 25, pp. 31-47.